

1  
2  
3 **Aliphatic Carbonyl Compounds (C<sub>8</sub>-C<sub>26</sub>) in Wintertime**  
4 **Atmospheric Aerosol in London, UK**  
5

6 **Ruihe Lyu<sup>1,2</sup>, Mohammed Salim Alam<sup>1</sup>, Christopher Stark<sup>1</sup>**

7 **Ruixin Xu<sup>1</sup>, Zongbo Shi<sup>1</sup>, Yinchang Feng<sup>2</sup> and Roy M. Harrison<sup>†\*1</sup>**  
8

9 **<sup>1</sup> Division of Environmental Health and Risk Management**  
10 **School of Geography, Earth and Environmental Sciences, University of**  
11 **Birmingham Edgbaston, Birmingham B15 2TT, UK**  
12

13 **<sup>2</sup> State Environmental Protection Key Laboratory of Urban Ambient Air**  
14 **Particulate Matter Pollution Prevention and Control, College of Environmental**  
15 **Science and Engineering**  
16 **Nankai University, Tianjin 300350, China**  
17  
18  
19

20 **† Also at: Department of Environmental Sciences / Centre of Excellence in Environmental**  
21 **Studies, King Abdulaziz University, PO Box 80203, Jeddah, 21589, Saudi Arabia.**  
22

23 **Corresponding authors:**

24 E-mail: [r.m.harrison@bham.ac.uk](mailto:r.m.harrison@bham.ac.uk) (Roy M. Harrison)  
25  
26

27 **ABSTRACT**

28 Three groups of aliphatic carbonyl compounds, the n-alkanals (C<sub>8</sub>-C<sub>20</sub>), n-alkan-2-ones (C<sub>8</sub>-C<sub>26</sub>) and  
29 n-alkan-3-ones (C<sub>8</sub>-C<sub>19</sub>) were measured in both particulate and vapour phases in air samples collected  
30 in London from January-April 2017. Four sites were sampled including two roof-top background  
31 sites, one ground-level urban background site and a street canyon location on Marylebone Road in  
32 central London. The n-alkanals showed the highest concentrations followed by the n-alkan-2-ones  
33 and the n-alkan-3-ones, the latter having appreciably lower concentrations. It seems likely that all  
34 compound groups have both primary and secondary sources and these are considered in the light of  
35 published laboratory work on the oxidation products of high molecular weight n-alkanes. All  
36 compound groups show relatively low correlation with black carbon and NO<sub>x</sub> in the background air  
37 of London, but in street canyon air heavily impacted by vehicle emissions, stronger correlations  
38 emerge especially for the n-alkanals. It appears that vehicle exhaust is likely to be a major contributor  
39 for concentrations of the n-alkanals whereas it is a much smaller contributor to the n-alkan-2-ones  
40 and n-alkan-3-ones. Other primary sources such as cooking or wood burning may be contributors for  
41 the ketones but were not directly evaluated. It seems likely that there is also a significant contribution  
42 from photo-oxidation of n-alkanes and this would be consistent with the much higher abundance of  
43 the n-alkan-2-ones relative to the n-alkan-3-ones if the formation mechanism were to be through  
44 oxidation of condensed phase alkanes. Vapour-particle partitioning fitted the Pankow model well for  
45 the n-alkan-2-ones but less well for the other compound groups, although somewhat stronger  
46 relationships were seen at the Marylebone Road site than at the background sites. The former  
47 observation gives support to the n-alkane-2-ones being a predominantly secondary product, whereas  
48 primary sources of the other groups are more prominent.

49 **Keywords:** Carbonyl compounds; n-alkanals; n-alkan-2-ones; n-alkan-3-ones; organic aerosol;  
50 partitioning;

## 51    **1.    INTRODUCTION**

52    Carbonyl compounds are classified as polar organic compounds, constituting a portion of the  
53    oxygenated organic compounds in atmospheric particulate matter (PM). Aliphatic carbonyl  
54    compounds are directly emitted into the atmosphere from primary biogenic and anthropogenic  
55    sources (Schauer et al., 2001, 2002a, b), as well as being secondary products of atmospheric  
56    oxidation of hydrocarbons (Chacon-Madrid et al., 2010; Zhang et al., 2015; Han et al., 2016).

57

58    The most abundant atmospheric carbonyls are methanal (formaldehyde) and ethanal (acetaldehyde),  
59    and many studies have described their emission sources and chemical formation in urban and rural  
60    samples (Duan et al., 2016). Long-chain aliphatic carbonyl compounds have been identified in PM  
61    and reported in few published papers (Gogou et al., 1996; Andreou and Rapsomanikis, 2009), and  
62    these compounds are considered to be formed from atmospheric oxidation processes affecting  
63    biogenic emissions of alkanes. Anthropogenic activity is also considered to be a significant  
64    contributor to the aliphatic carbonyls. Appreciable concentrations of aliphatic carbonyl compounds  
65    have been identified in emissions from road vehicles (Schauer et al., 1999a; 2002b), coal combustion  
66    (Oros and Simoneit, 2000), wood burning (Rogge et al., 1998) and cooking processes (Zhao et al.,  
67    2007a,b), spanning a wide range of molecular weights. Furthermore, chamber studies (Chacon-  
68    Madrid and Donahue, 2011; Algrim and Ziemann, 2016) have demonstrated that the aliphatic  
69    carbonyl compounds are very important precursors of secondary organic aerosol (SOA) when they  
70    react with OH radicals in the presence of NO<sub>x</sub>.

71

72 The oxidation of n-alkanes by hydroxyl radical is considered to be an important source of aliphatic  
73 carbonyl compounds. It was believed that the n-alkanals with carbon atoms numbering less than 20  
74 indicate oxidation of alkanes, whereas the higher compounds were usually considered to be of direct  
75 biogenic origin (Rogge et al., 1998). The homologues and isomers of n-alkanals and n-alkanones have  
76 been identified as OH oxidation products of n-alkanes in many chamber and flow tube studies (Zhang  
77 et al., 2015; Schilling Fahnstock et al., 2015; Ruehl et al., 2013; Yee et al., 2012), although not all  
78 studies identified the position of the carbonyl group. The commonly accepted oxidation pathways of  
79 n-alkanes generally divide into functionalization and fragmentation. Functionalization occurs when  
80 an oxygenated functional group ( $-\text{ONO}_2$ ,  $-\text{OH}$ ,  $-\text{C}=\text{O}$ ,  $-\text{C}(\text{O})\text{O}-$  and  $-\text{OOH}$ ) is added to a molecule,  
81 leaving the carbon skeleton intact. Alternatively, fragmentation involves C–C bond cleavage and  
82 produces two oxidation products with smaller carbon numbers than the reactant. The chamber studies  
83 of dodecane oxidation include observations of aldehydes and ketones as oxidation products (Schilling  
84 Fahnstock et al., 2015; Yee et al., 2012).

85

86 In London, with a high population density and a large number of diesel engine vehicles, the aliphatic  
87 hydrocarbons constitute an important fraction of ambient aerosols. Anthropogenic activities and  
88 secondary formation contribute to the emission and production of carbonyl compounds within the  
89 city. The objectives of the present study were the identification and quantification of aliphatic  
90 carbonyl compounds in particle and vapour samples collected in London from January to April 2017.  
91 This work has aided an understanding of the concentrations and secondary formation of carbonyls in  
92 the London atmosphere. Spatial and temporal variations of the studied carbonyl compounds were  
93 assessed and used to infer sources. One of the main objectives was to provide gas/particle partitioning

94 coefficients of identified carbonyls under realistic conditions. Diagnostic criteria were used to  
95 estimate the sources of identifiable atmospheric carbonyl compounds. Additionally, for the first time,  
96 concentrations of particulate and gaseous n-alkan-3-ones are reported.

97

## 98 **2. MATERIALS AND METHODS**

### 99 **2.1 Sampling Method and Site Characteristics**

100 Three sampling campaigns were carried out between 23 January and 18 April 2017 at four sampling  
101 sites (Figure 1) in London. The first campaign used two sampling sites, one located on the roof of a  
102 building (15 m above ground) of the Regent's University ( $51^{\circ}31'N$ ,  $-0^{\circ}9'W$ ), hereafter referred to as  
103 RU, sampled from 23 January 2017 to 19 February 2017, the other located on the roof (20 m above  
104 ground) of a building which belongs to the University of Westminster on the southern side of  
105 Marylebone Road (hereafter referred to as WM), sampled from 24 January 2017 to 20 February 2017.  
106 The third sampling site was located at ground level at Eltham ( $51^{\circ}27'N$ ,  $0^{\circ}4'E$ ), hereafter referred to  
107 as EL, sampled from 23 February 2017 to 21 March 2017, which is located in suburban south London,  
108 and the fourth sampling site was located at ground level on the southern side of Marylebone Road  
109 ( $51^{\circ}31'N$ ,  $-0^{\circ}9'W$ ), hereafter referred to as MR, sampled from 22 March 2017 to 18 April 2017.  
110 Marylebone Road is in London's commercial centre, and is an important thoroughfare carrying 80-  
111 90,000 vehicles per day through central London. The Regent's University site is within Regent's  
112 Park to the north of Marylebone Road. The Eltham site is in a typical residential neighbourhood, 22  
113 km from the MR site. Earlier work at the Marylebone Road and a separate Regent's Park site is  
114 described by Harrison et al. (2012).

115 The particle samples were collected on polypropylene backed PTFE filters (47 mm, Whatman) which  
116 preceded stainless steel sorbent tubes packed with 1cm quartz wool, 300 mg Carbograph 2TD 40/60  
117 (Markes International, Llantrisant, UK) and sealed with stainless-steel caps before and after sampling.  
118 Sampling took place for sequential 24-hour periods at a flow rate of 1.5 L min<sup>-1</sup> using an in-house  
119 developed automated sampler. Field blank filters and sorbent tubes were prepared for each site, and  
120 recovery efficiencies were evaluated. Adsorption tube breakthrough was tested in the field with six  
121 replicates of two tubes in series and for compounds of  $\geq C_{11}$  recovery exceeded 95% on the first tube.  
122 It was 85% for the C<sub>10</sub> compounds, and lower for C<sub>9</sub> and C<sub>8</sub> for which data are not reported. After  
123 the sampling, each filter was placed in a clean sealed petri dish, wrapped in aluminium foil and stored  
124 in the freezer at -18°C prior to analysis. Black carbon (BC) was simultaneously monitored during the  
125 sampling period at RU and WM sites using an aethalometer (Model AE22, Magee Science).  
126 Measurements of BC and NO<sub>x</sub> at MR and NO<sub>x</sub> at EL were provided by the national network sites of  
127 Marylebone Road, and Eltham (<https://uk-air.defra.gov.uk/>).

128

## 129 **2.2 Analytical Instrumentation**

130 The particle samples were analyzed using a 2D gas chromatograph (GC, 7890A, Agilent  
131 Technologies, Wilmington, DE, USA) equipped with a Zoex ZX2 cryogenic modulator (Houston,  
132 TX, USA). The first dimension was equipped with a SGE DBX5, non-polar capillary column (30.0  
133 m, 0.25 mm ID, 0.25 mm – 5.00% phenyl polysilphenylene-siloxane), and the second-dimension  
134 column equipped with a SGE DBX50 (4.00 m, 0.10 mm ID, 0.10 mm – 50.0% phenyl  
135 polysilphenylene-siloxane). The GC × GC was interfaced with a Bench-ToF-Select, time-of-flight  
136 mass spectrometer (ToF-MS, Markes International, Llantrisant, UK). The acquisition speed was 50.0

137 Hz with a mass resolution of >1200 fwhm at 70.0 eV and the mass range was 35.0 to 600 m/z. All  
138 data produced were processed using GC Image v2.5 (Zoex Corporation, Houston, US).

139

### 140 **2.3 Analysis of Samples**

141 Standards used in these experiments included 19 alkanes, C<sub>8</sub> to C<sub>26</sub> (Sigma-Aldrich, UK, purity  
142 >99.2%); 12 n-aldehydes, C<sub>8</sub> to C<sub>13</sub> (Sigma-Aldrich, UK, purity ≥95.0%), C<sub>14</sub> to C<sub>18</sub> (Tokyo  
143 Chemical Industry UK Ltd, purity >95.0%); and 10 2-ketones, C<sub>8</sub> to C<sub>13</sub> and C<sub>15</sub> to C<sub>18</sub> (Sigma-  
144 Aldrich, UK, purity ≥98.0%) and C<sub>14</sub> (Tokyo Chemical Industry UK Ltd, purity 97.0%).

145

146 The filters were spiked with 30.0 µL of 30.0 µg mL<sup>-1</sup> deuterated internal standards (dodecane-d<sub>26</sub>,  
147 pentadecane-d<sub>32</sub>, eicosane-d<sub>42</sub>, pentacosane-d<sub>52</sub>, triacontane-d<sub>62</sub>, butylbenzene-d<sub>14</sub>, nonylbenzene-  
148 2,3,4,5,6-d<sub>5</sub>, biphenyl-d<sub>10</sub>, p-terphenyl-d<sub>14</sub>; Sigma-Aldrich, UK) for quantification and then  
149 immersed in dichloromethane (DCM), and ultra-sonicated for 20.0 min at 20.0°C. The extract was  
150 filtered using a clean glass pipette column packed with glass wool and anhydrous Na<sub>2</sub>SO<sub>4</sub>, and  
151 concentrated to 50.0 µL under a gentle flow of nitrogen for analysis using GC × GC-ToF-MS. 1 µL  
152 of the extracted sample was injected in a split ratio 100:1 at 300°C. The initial temperature of the  
153 primary oven (80.0°C) was held for 2.0 min and then increased at 2.0 °C min<sup>-1</sup> to 210°C, followed by  
154 1.5 °C min<sup>-1</sup> to 325 °C. The initial temperature of the secondary oven (120°C) was held for 2.0 min  
155 and then increased at 3.0°C min<sup>-1</sup> to 200°C, followed by 2.00°C min<sup>-1</sup> to 300°C and a final increase  
156 of 1.0°C min<sup>-1</sup> to 330 °C to ensure all species passed through the column. The transfer line  
157 temperature was 330 °C and the ion source temperature was 280°C. Helium was used as the carrier



158 gas at a constant flow rate of 1.0 mL min<sup>-1</sup>. Further details of the instrumentation and data processing  
159 methods is given by Alam et al. (2016a,b).

160

161 The sorbent tubes were analyzed by an injection port thermal desorption unit (Unity 2, Markes  
162 International, Llantrisant, UK) and subsequently analyzed using GC × GC-ToF-MS. Briefly, the  
163 tubes were spiked with 1 ng of deuterated internal standard for quantification and desorbed onto the  
164 cold trap at 350°C for 15.0 min (trap held at 20.0°C). The trap was then purged onto the column in  
165 a split ratio of 100:1 at 350°C and held for 4.0 min. The initial temperature of the primary oven  
166 (90.0°C) was held for 2.0 min and then increased to 2.0°C min<sup>-1</sup> to 240°C, followed by 3.0°C min<sup>-1</sup>  
167 to 310°C and held for 5.0 min. The initial temperature of the secondary oven (40.0°C) was held for  
168 2.0 min and then increased at 3.0°C min<sup>-1</sup> to 250°C, followed by an increase of 1.5°C min<sup>-1</sup> to 315°C  
169 and held for 5.0 min. Helium was used as carrier gas for the thermally desorbed organic compounds,  
170 with a gas flow rate of 1.0 mL min<sup>-1</sup>.

171

## 172 *Qualitative analysis*

173 Compound identification was based on the GC×GC-TOFMS spectra library, NIST mass spectral  
174 library and in conjunction with authentic standards. Compounds within the homologous series for  
175 which standards were not available were identified by comparing their retention time interval between  
176 their homologues, and by comparison of mass spectra to the standards for similar compounds within  
177 the series, by comparison to the NIST mass spectral library and by the analysis of fragmentation  
178 patterns.

179

180 *Quantitative analysis*

181 An internal standard solution (outlined above) was added to the samples to extract prior to  
182 instrumental analysis. Five internal standards (pentadecane-d<sub>32</sub>, eicosane-d<sub>42</sub>, pentacosane-d<sub>52</sub>,  
183 triacontane-d<sub>62</sub>, nonylbenzene-2,3,4,5,6-d<sub>5</sub>) were used in the calculation of carbonyl compound  
184 concentrations.

185

186 The quantification for alkanes, aldehydes and 2-ketones was performed by the linear regression  
187 method using seven-point calibration curves (0.05, 0.10, 0.25, 0.50, 1.00, 2.00, 3.00 ng  $\mu\text{L}^{-1}$ )  
188 established between the authentic standards/internal standard concentration ratios and the  
189 corresponding peak area ratios. The calibration curves for all target compounds were highly linear  
190 ( $r^2 > 0.99$ , from 0.990 to 0.997), demonstrating the consistency and reproducibility of this method.

191 Limits of detection for individual compounds were typically in the range 0.04–0.12 ng  $\text{m}^{-3}$ . 3-ketones  
192 were quantified using the calibration curves for 2-ketones. This applicability of quantification of  
193 individual compounds using isomers of the same compound functionality (which have authentic  
194 standards) has been discussed elsewhere and has a reported uncertainty of 24% (Alam et al., 2018).

195 Alkan-2-ones and alkan-3-ones were not well separated by the chromatography. These were separated  
196 manually using the peak cutting tool, attributing fragments at  $m/z$  58 and 71 to 2-ketones and  $m/z$  72  
197 and 85 to 3-ketones.

198

199 Field and laboratory blanks were routinely analysed to evaluate analytical bias and precision. Blank  
200 levels of individual analytes were normally very low. Recovery efficiencies were determined by  
201 analyzing the blank samples spiked with standard compounds. Mean recoveries ranged between 78.0

202 and 102%. All quantities reported here have been corrected according to their recovery efficiencies.  
203 Detection limits are reported in Table S1.

204

### 205 **3. RESULTS AND DISCUSSION**

#### 206 **3.1 Mass Concentration of Particle-Bound Carbonyl Compounds**

207 The study of temporal and spatial variations of air pollutants can provide valuable information about  
208 their sources and atmospheric processing. The time series of particle-bound n-alkanals, n-alkan-2-  
209 ones, and n-alkan-3-ones are plotted in Figure 2. It is clear that the concentrations of n-alkanals varied  
210 substantially with date, and were always higher than n-alkanones at four sites. It is also clear from  
211 Figure 3 that concentrations were broadly similar at the background sites, RU, WM and EL, but are  
212 elevated, especially for the n-alkanals, at MR. This is strongly indicative of a road traffic source.

213

214 Carbonyls including n-alkanone homologues could result as fragmentation products from larger  
215 alkane precursors during gas-phase oxidation (Yee et al., 2012; Schilling Fahnestock et al., 2015) or  
216 as functionalized products from heterogeneous oxidation of particle-bound alkanes (Ruehl et al.,  
217 2013; Zhang et al., 2015). While carbonyl compounds are expected to be amongst first generation  
218 oxidation products of alkanes, product yields are not well known, and are highly dependent upon the  
219 chemical environment in which oxidation occurs. Yee et al. (2012) show substantial yields of mono-  
220 carbonyl product, the position of substitution undefined, in the low-NO<sub>x</sub> oxidation of n-dodecane.  
221 Ruehl et al. (2013) report the production of 2- through 14-octacosanone from the oxidation of  
222 octacosane, giving relative, but not absolute yields. Schilling Fahnestock et al. (2014) report

223 oxidation products of dodecane formed in both low-NO and high NO environments (<d.l and NO =  
224 97.5 ppb respectively). A singly substituted unfragmented ketone product is reported only from the  
225 low-NO oxidation, and in relatively low yield amongst many products. Lim and Ziemann (2009)  
226 propose a reaction scheme for the OH-initiated oxidation of alkanes in the presence of NO<sub>x</sub>. They  
227 express the view that first generation carbonyl formation is negligible at high NO concentrations for  
228 linear alkanes with C<sub>n</sub>>6 since reactions of an alkoxy radical with O<sub>2</sub> are too slow to compete with  
229 isomerisation, which leads ultimately to hydroxynitrate and hydroxycarbonyl products. Ziemann  
230 (2011) also shows a substantial yield of alkylnitrates from OH-initiated oxidation of n-alkanes from  
231 C<sub>10</sub>-C<sub>25</sub> in the presence of NO. The NO concentrations in the background air of London are <12  
232 ppb typically (UK-Air, 2018), and hence lie between the low and high NO environments of  
233 experiments in the literature, therefore most probably permitting some oxidation to proceed through  
234 pathways leading to first generation carbonyl products.

235

236 Figure 3 shows the average total concentrations of particle-bound 1-alkanals, n-alkan-2-ones, and  
237 n-alkan-3-ones from January to April at four measurement sites, and the particle and gaseous phase  
238 concentrations are detailed in the Table S2 (Supporting Information). Total n-alkanals was defined  
239 as the sum of particle-bound n-alkanals ranging from C<sub>8</sub> to C<sub>20</sub>. The particulate n-alkanals at the MR  
240 site accounted for 75.2% of the measured particle carbonyls with the average total concentration of  
241 682 ng m<sup>-3</sup>, and concentrations at the other sites were 167 ng m<sup>-3</sup> at EL, 117 ng m<sup>-3</sup> at WM and 82.6  
242 ng m<sup>-3</sup> at RU, accounting for 57.0%, 57.9% and 56.3% of the measured particulate carbonyls,  
243 respectively. The n-alkanals identified in this study differed substantially from those previously  
244 reported in samples collected from Crete (Gogou et al., 1996) and Athens (Andreou and

245 Rapsomanikis, 2009) in Greece. The n-alkanals from London presented narrower ranges of carbon  
246 numbers and a higher concentration than rural and urban samples from Crete. The concentrations of  
247 n-alkanal homologues (C<sub>8</sub>-C<sub>20</sub>) ranged from 5.50 to 141 ng m<sup>-3</sup> (average 52.0 ng m<sup>-3</sup>) at MR which  
248 were far higher than 1.48-28.6 ng m<sup>-3</sup> (average 6.44 ng m<sup>-3</sup>) at RU, 1.42-50.3 ng m<sup>-3</sup> (average 9.03  
249 ng m<sup>-3</sup>) at WM and 3.29-53.0 ng m<sup>-3</sup> (average 13.0 ng m<sup>-3</sup>) at EL (Table S1), unlike Crete where the  
250 concentrations were 0.9-3.7 ng m<sup>-3</sup> in rural (C<sub>15</sub>-C<sub>30</sub>) and 5.4-6.7 ng m<sup>-3</sup> in urban (C<sub>9</sub>-C<sub>22</sub>) samples,  
251 and the average concentration of all four sites was much higher than the 0.91 ng m<sup>-3</sup> measured in  
252 Athens (Andreou and Rapsomanikis, 2009) (C<sub>13</sub>-C<sub>20</sub>). This is a clear indication of a road traffic,  
253 most probably diesel source which is greater in London. Earlier work has clearly demonstrated a  
254 substantial elevation in traffic-generated pollutants at the Marylebone Road site, relative to  
255 background sites within London (Harrison and Beddows, 2017).

256

257 As part of the CARBOSOL project (Oliveira et al., 2007), air samples were collected in summer and  
258 winter at six rural sites across Europe. The particulate n-alkanals ranged from C<sub>11</sub> to C<sub>30</sub> with average  
259 total concentrations between 1.0 ng m<sup>-3</sup> and 19.0 ng m<sup>-3</sup>, with higher concentrations in summer than  
260 winter at all but one site. Maximum concentrations at all sites were in compounds >C<sub>22</sub> indicating a  
261 source from leaf surface abrasion products and biomass burning (Simoneit et al., 1967; Gogou et al.,  
262 1996). This far exceeds the C<sub>max</sub> (carbon number of the most abundant homologue) values seen in  
263 the particulate fraction at our sites.

264

265 The n-alkan-2-one homologues measured in London ranged from C<sub>8</sub> to C<sub>26</sub>, and the average total  
266 particulate fraction concentration was 58.5 ng m<sup>-3</sup> at RU, 75.1 ng m<sup>-3</sup> at WM, 112 ng m<sup>-3</sup> at EL and

267 186 ng m<sup>-3</sup> at MR, approximately accounting for 39.9% (RU), 37.0% (WM), 38.1% (EL) and 20.5%  
268 (MR) of the total particulate carbonyls, respectively (Figure 3). The published data from Greece  
269 indicated that the concentrations of n-alkan-2-ones were independent of the seasons, and an average  
270 of 5.40 ng m<sup>-3</sup> (C<sub>13</sub>-C<sub>29</sub>) was measured in August and 5.44 ng m<sup>-3</sup> in March at Athinas St, but 12.88  
271 ng m<sup>-3</sup> was measured in March at the elevated (20 m) AEDA site in Athens (Gogou et al., 1996).  
272 Concentrations in Crete for alkan-2-ones (C<sub>10</sub>-C<sub>31</sub>) were 0.4-2.1 ng m<sup>-3</sup> at the rural site and 1.9-2.6  
273 ng m<sup>-3</sup> at the urban site (Andreou and Rapsomanikis, 2009). The CARBOSOL project also  
274 determined concentrations of n-alkan-2-ones, between C<sub>14</sub> and C<sub>31</sub> with a C<sub>max</sub> at C<sub>28</sub> or C<sub>29</sub> at all  
275 but one site. Average concentrations ranged from 0.15 ng m<sup>-3</sup> (C<sub>17-29</sub>) to 3.35 (C<sub>14</sub>-C<sub>31</sub>), very much  
276 below the concentrations at our London sampling site. Cheng et al. (2006) measured concentrations  
277 of n-alkan-2-ones in the Lower Fraser Valley, Canada, in PM<sub>2.5</sub>. Samples collected in a road tunnel  
278 showed the highest concentrations, total 1.8-12.6 ng m<sup>-3</sup> for C<sub>10</sub>-C<sub>31</sub>, and were higher in daytime  
279 than nighttime. Concentrations at a forest site were 1.1-7.2 ng m<sup>-3</sup> without a diurnal pattern. Values  
280 of C<sub>max</sub> ranged from C<sub>16-17</sub> at the road tunnel to C<sub>27</sub> (secondary maximum) at the forest site. Values  
281 of CPI (Carbon Preference Index, defined in Section 3.2.1) averaged across sites from 1.00 to 1.34,  
282 giving little evidence for a substantial biogenic input from higher plant waxes. These data clearly  
283 suggest a road traffic source in London, but less influential than for the n-alkanals for which the  
284 increment at the roadside MR site is much greater.

285

286 The n-alkan-3-one homologues identified in the samples ranged from C<sub>8</sub> to C<sub>19</sub>, and the average of  
287 individual compound concentrations was 0.52 ng m<sup>-3</sup> at RU, 0.94 ng m<sup>-3</sup> at WM, 1.37 ng m<sup>-3</sup> at EL  
288 and 3.34 ng m<sup>-3</sup> at MR. The concentrations of n-alkan-3-ones at the four sites were lower than the n-

289 alkanals and n-alkan-2-ones, and MR had the highest average total mass concentrations  $39.4 \text{ ng m}^{-3}$   
290  $^3$ , followed by  $14.3 \text{ ng m}^{-3}$  at EL,  $10.4 \text{ ng m}^{-3}$  at WM and  $5.65 \text{ ng m}^{-3}$  at RU, respectively.

291

292 The isomeric carbonyls formed via OH-initiated heterogeneous reactions of n-octacosane ( $\text{C}_{28}$ )  
293 exhibit a pronounced preference at the 2-position of the molecule chain (Ruehl et al., 2013). The n-  
294 octacosan-2-ones have the highest relative yield (1.00), followed by n-octacosan-3-ones (0.50), while  
295 other isomeric carbonyl yields were lower than 0.20. The same results were found in the subsequent  
296 chamber studies of n-alkanes (Zhang et al., 2015) ( $\text{C}_{20}$ ,  $\text{C}_{22}$ ,  $\text{C}_{24}$  but not  $\text{C}_{18}$ ). The main probable  
297 reason was that a large fraction of  $\text{C}_{18}$  evaporated into the gas phase, and OH oxidation happened in  
298 the gas phase (homogeneous reaction). This may be supported by the evidence from previous studies  
299 (Kwok and Atkinson, 1995; Ruehl et al., 2013), which found that the isomeric distribution of  
300 oxidation products of n-alkanes depends upon whether the reaction occurs in the gas phase or at the  
301 particle surface (Kwok and Atkinson, 1995; Ruehl et al., 2013). The homogeneous gas-phase  
302 oxidation occurs fast, and H-abstraction by OH radicals occurs at all carbon sites. The fractions of  
303 the OH radical reaction by H atom abstraction from n-decane at the 1-, 2-, 3-, 4- and 5-positions are  
304 3.10%, 20.7%, 25.4%, 25.4%, and 25.4%, respectively, and the products from gas phase  
305 (homogeneous) reaction were generally in accord with structure-reactivity relationship (SRR)  
306 predictions (Kwok and Atkinson, 1995; Aschmann et al., 2001). Zhang et al. (2015) report on the  
307 competition between homogeneous and heterogeneous oxidation of medium to high molecular weight  
308 alkanes. They express the view that in the atmosphere, compounds typically classified as semi-  
309 volatile evaporate sufficiently rapidly that homogeneous gas phase oxidation is more rapid than  
310 oxidation in the condensed phase.

311 During the field experiment, the n-alkanal homologues were abundant in all samples, and this is  
312 probably attributable to the primary emission sources, including diesel vehicles (Schauer et al.,  
313 1999a), gasoline cars (Schauer et al., 2002b), wood burning (Rogge et al., 1998) and cooking aerosol  
314 (Schauer et al., 1999b). Correlations with other largely vehicle-generated pollutants (see later)  
315 support this interpretation. The particulate form of the n-alkane homologues (C<sub>14</sub>-C<sub>36</sub>) identified in  
316 the samples dominated for >C<sub>25</sub> and there was a significant particulate fraction (>60%) for all but the  
317 low MW n-alkanes (C<sub>14</sub>-C<sub>18</sub>) (unpublished data). The H-abstraction by OH radicals may therefore  
318 have been dominated by heterogeneous reactions generating the higher concentrations of n-alkan-2-  
319 ones than n-alkan-3-ones that were found in all samples. The ratio of n-alkan-2-ones/n-alkan-3-ones  
320 (C<sub>11</sub>-C<sub>18</sub>) with the same carbon atom number ranged from 2.35-11.3 at four measurement sites.  
321 Surprisingly, although the n-alkane (C<sub>11</sub>-C<sub>13</sub>) oxidation was expected to be dominated by  
322 homogeneous gas phase reactions, the n-alkan-2-one/n-alkan-3-one ratios were still greater than 2.00.  
323 The probable reason was that the lower molecular weight n-alkan-2-ones were significantly impacted  
324 by primary emission sources such as cooking (Zhao et al., 2007a,b). Another possible reason is that  
325 the n-alkan-2-one and n-alkan-3-one homologues with lower carbon atom numbers originated in part  
326 from the fragmental products of higher n-alkanes (Yee et al., 2012; Schilling Fahnstock et al., 2015),  
327 although fragmentation reactions would result mainly in the formation of alkanals, and are less likely  
328 to occur than isomerisation leading mostly to multifunctional products.

329

330 The ratios of n-alkan-2-ones/n-alkanes, n-alkan-3-ones/n-alkanes (with same carbon numbers) were  
331 calculated and are reported in Table S3. The n-alkan-3-ones with carbon numbers higher than C<sub>20</sub>  
332 were not identified in the samples, indicating that both the gas phase and heterogeneous reactions of



333 higher molecular weight n-alkanes were slow, the former probably due to the low vapour phase  
 334 presence of n-alkanes. The ratios of n-alkan-3-ones/n-alkanes at four measurement sites gradually  
 335 increased from C<sub>11</sub>, and then decreased from C<sub>17</sub>, while higher ratios of n-alkan-2-ones/n-alkanes were  
 336 observed in the range from C<sub>17</sub> to C<sub>22</sub>, probably indicating a shift from homogeneous gas phase  
 337 reactions to heterogeneous reactions with the increase of carbon numbers. The low ratios of n-alkan-  
 338 2-ones/n-alkanes with carbon numbers from C<sub>23</sub> to C<sub>26</sub> might be explained by the low diffusion rate  
 339 from the inner particle to the surface with the increasing carbon number of n-alkanes, even though  
 340 heterogeneous reactions would be the expected dominant pathway.

341

## 342 3.2 Sources of Carbonyl Compounds

### 343 3.2.1 Homologue distribution and carbon preference index (CPI)

344 Figure 4 shows the average concentrations, and molecular distributions of particle-bound carbonyl  
 345 compounds at the four sites. The values of carbon preference index (CPI) were calculated to estimate  
 346 the origin of carbonyl compounds, according to Bray and Evans (1961):

347

$$348 \text{ CPI} = \frac{1}{2} \left( \frac{\sum_4^m C_{2i+1}}{\sum_4^m C_{2i}} + \frac{\sum_4^m C_{2i+1}}{\sum_5^{m+1} C_{2i}} \right)$$

$$349 \text{ For n-alkanals and n-alkan-3-ones (m=9): CPI} = \frac{1}{2} \left( \frac{\sum \text{odd}(C_9-C_{19})}{\sum \text{even}(C_8-C_{18})} + \frac{\sum \text{odd}(C_9-C_{19})}{\sum \text{even}(C_{10}-C_{20})} \right)$$

$$350 \text{ For n-alkan-2-ones (m=12): CPI} = \frac{1}{2} \left( \frac{\sum \text{odd}(C_9-C_{25})}{\sum \text{even}(C_8-C_{24})} + \frac{\sum \text{odd}(C_9-C_{25})}{\sum \text{even}(C_{10}-C_{26})} \right)$$

351

352 where  $i$  takes values between 4 and  $m$ , and 5 and  $m$  as in the equation, and

353  $m = 9$  for n-alkanal and n-alkan-3-ones

354  $m = 12$  for n-alkan-2-ones

355 The carbon number of the homologue of highest concentration ( $C_{\max}$ ) can be indicative of the source.  
356 Table. 1 presents the CPI and  $C_{\max}$  of particle-bound carbonyl compounds calculated in the current  
357 and other studies. A CPI of  $\leq 1$  is an indication of an anthropogenic source, while a CPI of 1-5  
358 shows a mixture of anthropogenic and biogenic sources and a CPI  $> 5$  suggests a biogenic (plant wax)  
359 source.

360

361 The n-alkanes which are potential precursors of the oxygenates described typically showed two  $C_{\max}$   
362 values, the first at  $C_{13}$  (the lowest MW compound measured), and at  $C_{23}$ . The CPI values for the  
363 n-alkanes were between 0.97-1.02 at the four measurements sites (unpublished data).

364

365 According to the low CPI (0.41-1.07) at the four sites, the n-alkanal homologues with carbon number  
366 from  $C_8$  to  $C_{20}$  mainly originate from anthropogenic emissions or OH oxidation of fossil-derived  
367 hydrocarbons. The particle-bound n-alkanals exhibited a similar distribution of carbon number from  
368 January to April at four sites, and they had the same  $C_{\max}$  at  $C_8$  with concentration  $28.6 \text{ ng m}^{-3}$  at  
369 RU,  $50.3 \text{ ng m}^{-3}$  at WM,  $53.0 \text{ ng m}^{-3}$  at EL and  $141 \text{ ng m}^{-3}$  at MR, respectively. This compound may  
370 be a fragmentation product, oxidation product or primary emission. In addition, the distribution of  
371 n-alkanals had a second concentration peak at  $C_{15}$  (MR) and  $C_{18}$  (RU, WM, and EL). The  $C_{18}$   
372 compound was observed accounting for the highest percentage of the total mass of n-alkanals in  
373 some rural aerosol samples (Gogou et al., 1996) in Crete. Andreou and Rapsomanikis reported the  
374  $C_{\max}$  as  $C_{15}$  or  $C_{17}$  in Athens (Andreou and Rapsomanikis, 2009) and attributed this to the oxidation

375 of n-alkanes. However, a  $C_{max}$  at  $C_{26}$  or  $C_{28}$  in urban Crete (Gogou et al., 1996) was observed,  
376 suggestive of biogenic input. The homologue distribution and CPI of n-alkanals in this study differed  
377 from those previous reports, and demonstrated weak biogenic input and a strong impact of  
378 anthropogenic activities in the London samples.

379

380 In this study, n-alkan-2-ones have similar homologue distributions and  $C_{max}$  ( $C_{19}$  or  $C_{20}$ ) (Table 2)  
381 at RU, WM and EL sites, and the total concentration from  $C_{16}$  to  $C_{23}$  accounts for 76.0%, 76.1% and  
382 68.0% of  $\sum$ n-alkan-2-ones, respectively. The CPI values for n-alkan-2-ones ranged from 0.57 to  
383 1.23 at the RU, MR and WM sites and were not indicative of major biogenic input, and were  
384 considered to mainly originate from anthropogenic activities and OH oxidation of anthropogenic n-  
385 alkanes. It is however notable that the CPI values for both the 2-ketones and 3-ketones exceed  
386 those for the alkanals (see Table 1), suggesting a contribution from contemporary biogenic sources,  
387 possibly wood smoke and cooking. At EL, the CPI of 1.57 is clearly indicative of a biogenic  
388 contribution in suburban south London. A difference was observed at the MR site, the n-alkan-2-  
389 ones with carbon atoms numbering from  $C_{12}$  to  $C_{18}$  accounting for 72.0% of  $\sum$ n-alkan-2-ones, with  
390 the  $C_{max}$  being at  $C_{16}$ . These data suggest a contribution of primary emissions from traffic at MR,  
391 but a dominant background, probably substantially secondary, at the other sites. The  $C_{max}$  of n-alkan-  
392 3-ones was at  $C_{16}$  at the MR site, at EL,  $C_{max} = C_{16}$ , WM,  $C_{max} = C_{17}$  and at RU,  $C_{max} = C_{17}$ ,  
393 respectively.

394

395

### 396 3.2.2 The ratios of n-alkanes/n-alkanals

397 Diesel engine emission studies have been conducted previously in our group; details of the engine set  
398 up and exhaust sampling system are given elsewhere (Alam et al., 2016b). Briefly, the steady-state  
399 diesel engine operating conditions were at a load of 5.90 bar mean effective pressure (BMEP) and a  
400 speed of 1800 revolutions per minute (RPM), and samples (n=14) were collected both before a diesel  
401 oxidation catalyst (DOC) and after a diesel particulate filter (DPF). The n-alkanes (C<sub>12</sub> - C<sub>37</sub>) and 1-  
402 alkanals (C<sub>9</sub> - C<sub>18</sub>) were quantified in the particle samples, while n-alkanones were not identified  
403 because their concentrations were lower than the limits of (detection 0.01–0.15 ng m<sup>-3</sup>). The emission  
404 concentrations of n-alkanals ranged from 7.10 to 53.2 µg m<sup>-3</sup> (before DOC) and 1.20 to 11.5 µg m<sup>-3</sup>  
405 (after DPF), respectively, and the ratios of alkanes/alkanals (C<sub>13</sub>-C<sub>18</sub>) with the same carbon atom  
406 numbers ranged from 0.15 to 0.23 (before DOC) and 0.52 to 7.60 (after DPF). The n-alkane/n-alkanal  
407 (C<sub>13</sub>-C<sub>18</sub>) ratio at MR ranged from 0.30 to 5.7, while average ratios of 14.9 (RU), 11.5 (WM) and  
408 14.7 (EL) were obtained, respectively. The similarity of the n-alkanes/n-alkanal ratio between MR  
409 and the engine studies (after DPF) strongly suggests that diesel vehicle emissions were the main  
410 source of alkanals at MR. The higher ratios at the other sites may be due to greater air mass aging and  
411 loss of alkanals due to their higher reactivity (Chacon-Madrid and Donahue, 2011; Chacon-Madrid  
412 et al., 2010).

413

414 The emission factors of total alkanes from diesel engines are reported to be 7 times greater than  
415 gasoline engines (Perrone et al., 2014), with n-alkanals with carbon atoms numbering lower than C<sub>11</sub>  
416 being quantified in the exhaust from gasoline engines (Schauer et al., 2002b; Gentner et al., 2013).  
417 The n-alkane/n-alkanal (C<sub>8</sub>-C<sub>10</sub>) ratio with the same carbon numbers ranged from 5.60 to 14.3

418 (Schauer et al., 2002b), suggesting that gasoline combustion may be another potential source of  
419 atmospheric n-alkanal.

420

### 421 **3.2.3 Correlation analysis**

422 Insights into the sources of carbonyls can be gained from intra-site correlation analysis with black  
423 carbon (BC) and NO<sub>x</sub>. This is more informative than comparisons between sites when sampling did  
424 not take place simultaneously, as concentrations are strongly affected by weather conditions, making  
425 inter-site comparisons difficult to interpret. In London, both black carbon and NO<sub>x</sub> arise very  
426 substantially from diesel vehicle emissions (Liu et al., 2014; Harrison et al., 2012; Harrison and  
427 Beddows, 2017), and hence these are good measures of road traffic activity. The concentrations of  
428 BC were simultaneously determined by the online instruments during the sampling periods, with the  
429 average concentrations of 1.34, 1.94 and 3.58 µg m<sup>-3</sup> at the RU, WM and MR sites, respectively.  
430 The data for NO<sub>x</sub> were provided by the national network sites, with the average concentrations of  
431 23.4 and 202 µg m<sup>-3</sup> at the EL and MR sites, respectively. At the MR site, the concentrations of BC  
432 and NO<sub>x</sub> averaged 5.00 µg m<sup>-3</sup> and 281 µg m<sup>-3</sup> when southerly winds were dominant compared to  
433 2.60 and 128 µg m<sup>-3</sup> for northerly winds. All correlations were carried out with the sum of particle  
434 and vapour phases for the carbonyl compounds, and strong ( $r^2 = 0.87$ ) and weak ( $r^2 = 0.12$ )  
435 correlations between BC and NO<sub>x</sub> were obtained when the southerly and northerly winds were  
436 prevalent at MR, respectively. Marylebone Road is a street canyon site where a vortex circulation is  
437 established by the wind. The effect is that on northerly wind sectors the sampling site on the southern  
438 side of the road samples near-background air, while on southerly wind sectors, the traffic pollution  
439 is carried to the sampling site, leading to elevated pollution levels affected heavily by the traffic

440 emissions. The strong correlation between BC and NO<sub>x</sub> with southerly wind sectors is a reflection  
441 of their emission from road traffic. In addition, the correlations between n-alkanals (C<sub>8</sub>-C<sub>20</sub>) and BC,  
442 and between n-alkanals (C<sub>8</sub>-C<sub>20</sub>) and NO<sub>x</sub> were calculated to assess the contribution of vehicular  
443 emissions (Table S4). The results showed that the correlations ( $r^2$ ) between n-alkanals and BC  
444 gradually decreased from 0.61 (C<sub>9</sub>) to 0.34 (C<sub>20</sub>) at MR when the southerly winds were prevalent,  
445 indicating that the distribution of n-alkanals, and especially the lower MW compounds, was  
446 significantly impacted by the vehicular exhaust emissions. The average correlations at MR  
447 (southerly winds) between n-alkanals and BC, and between n-alkanals and NO<sub>x</sub> were  $r^2 = 0.47$  and  
448  $r^2 = 0.32$ , respectively. These moderate correlations demonstrated that the vehicular emissions were  
449 a source of n-alkanals at MR, and contribute to the high background concentrations of n-alkanals in  
450 London. The other probable sources of n-alkanals include cooking emissions, wood burning,  
451 photooxidation of hydrocarbons and industrial emissions. Poorer correlations between n-alkanals  
452 and BC (average  $r^2 = 0.15$ ), and between n-alkanals and NO<sub>x</sub> (average  $r^2 = 0.15$ ) were observed at  
453 MR in the north London background air sampled when northerly winds were prevalent. There were  
454 very weak correlations (average  $r^2 < 0.10$ ) between n-alkanals and BC, and between n-alkanals and  
455 NO<sub>x</sub> at the RU, WM and EL sites, which may be attributable to the high chemical reactivity of n-  
456 alkanals. High concentrations of furanones ( $\gamma$ -lactones) are generated via the photo-oxidation  
457 reaction of n-alkanals (Alves et al., 2001), and the total concentrations (particle and gas) were up to  
458 376, 279, 347 and 318 ng m<sup>-3</sup> at RU, WM, WL, and MR, respectively for the sum of furanone  
459 homologues (from 5-propyldihydro-2(3H)-furanone to 5-tetradecyldihydro-2(3H)-furanone).

460

461 The relationships ( $r^2$  values) between BC and  $\text{NO}_x$  and the n-alkan-2-ones were low at all sites, but  
462 notably higher with southerly winds at MR (average  $r^2 = 0.33$  and  $0.35$  for BC and  $\text{NO}_x$  respectively)  
463 than for northerly winds ( $r^2 = 0.16$  and  $0.03$  respectively). This is strongly suggestive of a  
464 contribution from vehicle exhaust to n-alkan-2-one concentrations, but smaller than that for n-  
465 alkanals. In the case of the n-alkan-3-ones, correlations averaged  $r^2 = 0.25$  with BC and  $r^2 = 0.21$  for  
466  $\text{NO}_x$  in southerly winds, compared to  $r^2 = 0.08$  and  $r^2 = 0.05$  respectively for northerly winds. This  
467 is also suggestive of a small, but not negligible contribution of vehicle emissions to n-alkan-3-ones.  
468 The very low correlations observed in background air for both n-alkan-2-ones and n-alkan-3-ones  
469 with BC and  $\text{NO}_x$  are suggestive of the importance of non-traffic sources, probably including  
470 oxidation of n-alkanes. Both compound groups were below detection limit in the analyses of diesel  
471 exhaust. The considerable predominance of n-alkan-2-one over n-alkan-3-one concentrations may  
472 be indicative of a formation pathway from oxidation of condensed phase n-alkanes, but this is  
473 speculative as primary emissions may be dominant.

474

### 475 3.3 Gas and Particle Phase Partitioning

476 The partitioning coefficient  $K_p$  between particles and vapour ( $\geq C_{10}$ ) was calculated in this study  
477 according to the following equation defined by Pankow (1994):

478

$$479 K_p = \frac{C_p}{C_g * TSP}$$

480

481 Where,  $C_p$  and  $C_g$  ( $\mu\text{g m}^{-3}$ ) are the concentration of the compounds in the particulate phase and  
482 gaseous phase, respectively. TSP is the concentration of total suspended particulate matter ( $\mu\text{g m}^{-3}$ ),

483 which was estimated from the PM<sub>10</sub> concentration (PM<sub>10</sub>/TSP = 0.80), and daily average PM<sub>10</sub>  
484 concentrations were taken from the national network sites (see Table S5). The partitioning  
485 coefficients  $K_p$  calculated from our data and the percentages in the particulate form are presented in  
486 Table 2. For the three types of carbonyls, the n-alkanals >C<sub>16</sub>, n-alkan-2-ones >C<sub>19</sub>, and n-alkan-3-  
487 ones > C<sub>18</sub> the vapour concentrations were below detection limit, and the partitioning into the  
488 particulate phase gradually increased from C<sub>8</sub> to high molecular weight compounds.

489

490 Log  $K_p$  was regressed against vapour pressure ( $VP_T$ ) for the relevant temperature derived from  
491 UManSysProp (<http://umansysprop.seaes.manchester.ac.uk/>) according to the following equation:

492

$$493 \text{Log } K_p = m \log(VP_T) + b$$

494

495 The calculated log  $K_p$  versus log ( $VP_T$ ) for the three types of carbonyls was calculated for each day,  
496 and the results appear in the Table S6. Data from four sites were over the temperature range 0.4–  
497 15.3 °C. A good fit to the data for n-alkan-2-ones ( $r^2 = 0.55$ – $0.94$  at RU,  $0.64$ – $0.93$  at WM,  $0.45$ –  
498  $0.94$  EL and  $0.36$ – $0.88$  at MR) was obtained. It is notable that the fit to the regression equation as  
499 indicated by the  $r^2$  value is appreciably higher at the MR site than at the other sites, especially in the  
500 case of the alkan-3-ones (Table S6). This is not easily explained, except perhaps by an increased  
501 particle surface area at the MR site which may enhance the kinetics of gas-particle exchange, leading  
502 to partitioning which is closer to equilibrium.

503



504 According to theory, the gradient of the plot of  $\log K_P$  versus  $\log (VP_T)$  should be -1 (Pankow,  
505 1994). However, many measurement datasets for a number of semi-volatile compound groups  
506 including n-alkanes (Cincinelli et al., 2007; Karanasiou et al., 2007; Mandalakis et al., 2002) and  
507 PAH (Callen et al., 2008; Wang et al., 2011; Ma et al., 2011; Mandalakis et al., 2002) show a range  
508 of values, often around -0.5, but ranging to below -1, and in some cases positive. Callen et al.,  
509 (2008) discuss the reasons for deviation from a value of -1, which include a lack of equilibrium,  
510 absorption into the organic matter (shallower than -0.6), adsorption processes (steeper than -1), and  
511 the averaging of conditions across a range of temperatures during a sampling period.

512

513 Our data for alkan-2-ones show high  $r^2$  values and values of gradient (m) in the range of the  
514 literature for other groups of semi-volatile compounds. Average gradients at the four sites ranged  
515 from -0.46 to -0.26. The alkan-3-ones show generally considerably lower values of  $r^2$  and average  
516 values of gradient at the four sites of -0.43 to -0.23. This poorer correlation could be the result of  
517 lower analytical precision. The n-alkanals show still lower values of  $r^2$ , and more variable and  
518 shallower values of slope. Mean slopes for the four sites ranged from -0.23 to -0.16. There were  
519 no positive daily values. The lower  $r^2$  may be a result of disequilibrium for the alkanals which are  
520 dominated by primary emissions, and are also more reactive. It might also reflect a role for aqueous  
521 aerosol as an absorbing medium for these compounds containing a significant polar moiety, which  
522 would lead to deviations from the Pankow (1994) theory, and more variable behaviour as the  
523 availability of aqueous particles into which to partition would depend upon relative humidity, which  
524 is itself highly variable.

525

526 Samples were collected over 24-hour periods and hence the diurnal variation of temperature may be  
527 relevant. Temperature data were taken from Heathrow Airport to the west of London and did not  
528 show large diurnal fluctuations, so this should not be a major factor. The average diurnal  
529 temperature range based upon hourly data was 6.9°C.

530

531 The lower molecular weight n-alkanals show a much higher percentage in the condensed phase than  
532 the ketone groups (Table 2).

533

534 This greater propensity to partition into the particles is unexpected, as the vapour pressures of the  
535 alkanals are very similar to those of the ketones. It might possibly reflect a greater affinity of the  
536 alkanals for solvation by water molecules, leading to increased partition into aqueous aerosol.

537

#### 538 **4. CONCLUSIONS**

539 Three groups of carbonyl compounds were determined in the particle and gaseous phase in London  
540 and concentrations are reported for n-alkanals (C<sub>8</sub>-C<sub>20</sub>), n-alkan-2-ones (C<sub>8</sub>-C<sub>26</sub>) and n-alkan-3-ones  
541 (C<sub>8</sub>-C<sub>19</sub>). The Marylebone Road site has the highest concentration of particle-bound n-alkanals, and  
542 the average total concentration was up to 682 ng m<sup>-3</sup>, followed by 167 ng m<sup>-3</sup> at EL, 117 ng m<sup>-3</sup> at  
543 WM and 82.6 ng m<sup>-3</sup> at RU. The particulate n-alkanals were abundant in all samples at all four  
544 measurement sites, accounting for more than 56.3% of total particle carbonyls. In addition, the  
545 average total particle concentrations of n-alkan-2-ones and n-alkan-3-ones at four measurement sites  
546 were in the range of 58.5-186 ng m<sup>-3</sup> and 5.65-39.4 ng m<sup>-3</sup>, respectively. Diagnostic criteria,

547 including molecular distribution, CPI,  $C_{\max}$ , ratios and correlations, were used to assess the sources  
548 and their contributions to carbonyl compounds. The three groups of carbonyls have similar  
549 molecular distributions and  $C_{\max}$  values at the four measurement sites, and their low CPI values  
550 (0.41-1.57) at the four sites indicate a weak biogenic input during sampling campaigns. Heavily  
551 traffic-influenced air and urban background air were measured at the MR site when southerly and  
552 northerly winds were prevalent respectively; correlations of  $r^2 = 0.47$  and  $r^2=0.32$  were obtained  
553 between n-alkanals and BC, and between between n-alkanals and  $\text{NO}_x$ , respectively in southerly  
554 winds. Vehicle emissions appear to be an important source of n-alkanals, which is confirmed by the  
555 similar ratios of n-alkanes/n-alkanals measured at MR (0.30-5.75) and in diesel engine exhaust  
556 studies (0.52-7.6), resulting in a high background concentration in London. In addition, the OH-  
557 initiated heterogeneous reactions of n-alkanes appear to be important sources of n-alkanones, even  
558 though weak contributions from vehicular exhaust emissions were suggested by correlation analysis  
559 with BC and  $\text{NO}_x$  in southerly winds at MR. Anthropogenic primary sources such as cooking  
560 (Abdullahi et al., 2013) may account for a proportion of the alkan-2-one and alkan-3-one  
561 concentrations measured in London, in addition to the secondary contribution from alkane oxidation.  
562 Any contribution from cooking or wood combustion is likely to be small, or the CPI would be greater.  
563  
564 In addition, the partitioning coefficients of carbonyls were determined from the relative proportions  
565 of the particle and gaseous phases of individual compounds, and generally showed a better fit at MR  
566 than at the other three sites. Fits to the Pankow (1994) model were best for alkan-2-ones and this  
567 most likely reflects the slow formation of the alkan-2-ones as secondary constituents, closer to phase

568 equilibrium than the predominantly emitted and more reactive alkanals which would be spatially  
569 more variable.

570

## 571 **ACKNOWLEDGEMENTS**

572 Primary collection of samples took place during the FASTER project which was funded by the  
573 European Research Council (ERC-2012-AdG, Proposal No. 320821). The authors would also like  
574 to thank the China Scholarship Council (CSC) for support to R.L., and the Natural Environment  
575 Research Council for support under the Air Pollution and Human Health (APHH) programme  
576 (NE/N007190/1).

577 **REFERENCE**

578

579 Abdullahi, K.L., Delgado-Saborit, J.M., and R.M. Harrison: Emissions and indoor concentrations  
580 of particulate matter and its specific chemical components from cooking: A review, *Atmos.*  
581 *Environ.*, 71, 260-294, <http://dx.doi.org/10.1016/j.atmosenv.2013.01.061>, 2013.

582

583 Alam, M. S., Stark, C., and Harrison, R. M.: Using variable ionization energy time-of-flight mass  
584 spectrometry with comprehensive GC×GC to identify isomeric species, *Anal. Chem.*, 88, 4211-  
585 4220, <http://www.doi.org/10.1021/acs.analchem.5b03122>, 2016a.

586

587 Alam, M. S., Zeraati-Rezaei, S., Stark, C. P., Liang, Z., Xu, H., and Harrison, R. M.: The  
588 characterisation of diesel exhaust particles - composition, size distribution and partitioning,  
589 *Faraday. Discuss.*, 189, 69-84, <http://www.doi.org/10.1039/C5FD00185D>, 2016b.

590

591 Alam, M. S., Zeraati-Rezaei, S., Liang, Z., Stark, C., Xu, H., MacKenzie, A. R., and Harrison, R.  
592 M.: Mapping and quantifying isomer sets of hydrocarbons ( $\geq C_{12}$ ) in diesel exhaust, lubricating oil  
593 and diesel fuel samples using GC×GC-ToF-MS, *Atmos. Meas. Tech.*, 11, 3047,  
594 <https://doi.org/10.5194/amt-11-3047-2018>, 2018.

595

596 Algrim, L. B., and Ziemann, P. J.: Effect of the Keto Group on yields and composition of organic  
597 aerosol formed from OH radical-initiated reactions of ketones in the presence of NO<sub>x</sub>, *J. Phys.*  
598 *Chem. A.*, 120, 6978-6989, <http://www.doi.org/10.1021/acs.jpca.6b05839>, 2016.

599

600 Alves, C., Pio, C., and Duarte, A.: Composition of extractable organic matter of air particles from  
601 rural and urban Portuguese areas, *Atmos. Environ.*, 35, 5485-5496, [https://doi.org/10.1016/S1352-](https://doi.org/10.1016/S1352-2310(01)00243-6)  
602 [2310\(01\)00243-6](https://doi.org/10.1016/S1352-2310(01)00243-6), 2001.

603

604 Andreou, G., and Rapsomanikis, S.: Origins of n-alkanes, carbonyl compounds and molecular  
605 biomarkers in atmospheric fine and coarse particles of Athens, Greece, *Sci. Total. Environ.*, 407,  
606 5750-5760, <http://dx.doi.org/10.1016/j.scitotenv.2009.07.019>, 2009.

607

608 Aschmann, S. M., Arey, J., and Atkinson, R.: Atmospheric chemistry of three C<sub>10</sub> alkanes, *J. Phys.*  
609 *Chem. A.*, 105, 7598-7606, <http://www.doi.org/10.1021/jp010909j>, 2001.

610

611 Bray, E., and Evans, E.: Distribution of n-paraffins as a clue to recognition of source beds,  
612 *Geochim. Cosmochim. Ac.*, 22, 2-15, [https://doi.org/10.1016/0016-7037\(61\)90069-2](https://doi.org/10.1016/0016-7037(61)90069-2), 1961.

613

614 Callen, M. S., de la Cruz, M. T., Lopez, J. M., Murillo, R., Navarro, M. V., and Mastral, A. M.:  
615 Some inferences on the mechanism of atmospheric gas/particle partitioning of polycyclic aromatic  
616 hydrocarbons (PAH) at Zaragoza (Spain), *Chemosphere*, 73, 1357-1365, 2008.

617

618 Chacon-Madrid, H., and Donahue, N.: Fragmentation vs. functionalization: chemical aging and  
619 organic aerosol formation, *Atmos. Chem. Phys.*, 11, 10553-10563, [https://doi.org/10.5194/acp-11-](https://doi.org/10.5194/acp-11-10553-2011)  
620 [10553-2011](https://doi.org/10.5194/acp-11-10553-2011), 2011.

621 Chacon-Madrid, H. J., Presto, A. A., and Donahue, N. M.: Functionalization vs. fragmentation: n-  
622 aldehyde oxidation mechanisms and secondary organic aerosol formation, *Phys. Chem. Chem.*  
623 *Phys.*, 12, 13975-13982, <http://www.doi.org/10.1039/C0CP00200C>, 2010.

624 Cheng, Y., Li, S.-M., Leithead, A., and Brook, J. R.: Spatial and diurnal distributions of n-alkanes  
625 and n-alkan-2-ones on PM 2.5 aerosols in the Lower Fraser Valley, Canada, *Atmos. Environ.*, 40,  
626 2706-2720, <https://doi.org/10.1016/j.atmosenv.2005.11.066>, 2006.

627

628 Cincinelli, A., Del Bubba, M., Martellini, T., Gambaro, A., and Lepri, L.: Gas-particle  
629 concentration and distribution of n-alkanes and polycyclic aromatic hydrocarbons in the atmosphere  
630 of Prato (Italy), *Chemosphere*, 68, 472-478, 2007.

631

632 Duan, H., Liu, X., Yan, M., Wu, Y., and Liu, Z.: Characteristics of carbonyls and volatile organic  
633 compounds (VOCs) in residences in Beijing, China, *Front. Env. Sci. Eng.*, 10, 73-84,  
634 <http://www.doi.org/10.1007/s11783-014-0743-0>, 2016.

635

636 Gentner, D. R., Worton, D. R., Isaacman, G., Davis, L. C., Dallmann, T. R., Wood, E. C., Herndon,  
637 S. C., Goldstein, A. H., and Harley, R. A.: Chemical composition of gas-phase organic carbon  
638 emissions from motor vehicles and implications for ozone production, *Environ. Sci. Technol.*, 47,  
639 11837-11848, <http://www.doi.org/10.1021/es401470e>, 2013.

640

641 Gogou, A., Stratigakis, N., Kanakidou, M., and Stephanou, E. G.: Organic aerosols in Eastern  
642 Mediterranean: components source reconciliation by using molecular markers and atmospheric back  
643 trajectories, *Org. Geochem.*, 25, 79-96, [https://doi.org/10.1016/S0146-6380\(96\)00105-2](https://doi.org/10.1016/S0146-6380(96)00105-2), 1996.

644

645 Han, Y., Kawamura, K., Chen, Q., and Mochida, M.: Formation of high-molecular-weight  
646 compounds via the heterogeneous reactions of gaseous C8–C10 n-aldehydes in the presence of  
647 atmospheric aerosol components, *Atmos. Environ.*, 126, 290-297,  
648 <http://dx.doi.org/10.1016/j.atmosenv.2015.11.050>, 2016.

649

650 Harrison, R., Dall'Osto, M., Beddows, D., Thorpe, A., Bloss, W., Allan, J., Coe, H., Dorsey, J.,  
651 Gallagher, M., and Martin, C.: Atmospheric chemistry and physics in the atmosphere of a  
652 developed megacity (London): an overview of the REPARTEE experiment and its conclusions,  
653 *Atmos. Chem. Phys.*, 12, 3065-3114, <https://doi.org/10.5194/acp-12-3065-2012>, 2012.

654

655 Harrison, R. M., and Beddows, D. C.: Efficacy of recent emissions controls on road vehicles in  
656 Europe and implications for public health, *Sci. Rep-UK.*, 7, 1152,  
657 <http://www.doi.org/10.1038/s41598-017-01135-2>, 2017.

658

659 Karanasiou, A. A., Sitaras, I. E., Siskos, P. A., and Eleftheriadis, K.: Size distribution and sources  
660 of trace metals and n-alkanes in the Athens urban aerosol during summer, *Atmos. Environ.*, 41,  
661 2368-2381, 2007.

662

663 Kwok, E. S., and Atkinson, R.: Estimation of hydroxyl radical reaction rate constants for gas-phase  
664 organic compounds using a structure-reactivity relationship: an update, *Atmos. Environ.*, 29, 1685-  
665 1695, [https://doi.org/10.1016/1352-2310\(95\)00069-B](https://doi.org/10.1016/1352-2310(95)00069-B), 1995.

666  
667 Lim, Y. B., and Ziemann, P.J.: Chemistry of secondary organic aerosol formation from OH  
668 radical-initiated reactions of linear, branched, and cyclic alkanes in the presence of NO<sub>x</sub>, *Aerosol*  
669 *Sci. Technol.*, 43, 604-619, <https://doi.org/10.1080/02786820902802567>, 2009.  
670  
671 Liu, D., Allan, J., Young, D., Coe, H., Beddows, D., Fleming, Z., Flynn, M., Gallagher, M.,  
672 Harrison, R., and Lee, J.: Size distribution, mixing state and source apportionments of black carbon  
673 aerosols in London during winter time, *Atmos. Chem. Phys.*, 14, [https://doi.org/10.5194/acp-14-](https://doi.org/10.5194/acp-14-10061-2014)  
674 10061-2014, 2014.  
675  
676 Ma, W.-L., Sun, D.-Z., Shen, W.-G., Yang, M., Qi, H., Liu, L.-Y., Shen, J.-M., and Li, Y.-F.:  
677 Atmospheric concentrations, sources and gas-particle partitioning of PAHs in Beijing after the 29th  
678 Olympic Games, *Environ. Pollut.*, 159, 1794-1801, 2011.  
679  
680 Mandalakis, M., Tsapakis, M., Tsoga, A., and Stephanou, E. G.: Gas-particle concentrations and  
681 distribution of aliphatic hydrocarbons, PAHs, PCBs and PCDD/Fs in the atmosphere of Athens  
682 (Greece), *Atmos. Environ.*, 36, 4023-4034, 2002.  
683  
684 Oliveira, T. S., Pio, C., Alves, C. A., Silvestre, A. J., Evtyugina, M., Afonso, J., Fialho, P., Legrand,  
685 M., Puxbaum, H., and Gelencsér, A.: Seasonal variation of particulate lipophilic organic  
686 compounds at nonurban sites in Europe, *J. Geophys. Res-Atmos.*, 112,  
687 <https://doi.org/10.1029/2007JD008504> 2007.  
688  
689 Oros, D. R., and Simoneit, B. R. T.: Identification and emission rates of molecular tracers in coal  
690 smoke particulate matter, *Fuel.*, 79, 515-536, [http://dx.doi.org/10.1016/S0016-2361\(99\)00153-2](http://dx.doi.org/10.1016/S0016-2361(99)00153-2),  
691 2000.  
692  
693 Pankow, J. F.: An absorption model of gas/particle partitioning of organic compounds in the  
694 atmosphere, *Atmos. Environ.*, 28, 185-188, [https://doi.org/10.1016/1352-2310\(94\)90093-0](https://doi.org/10.1016/1352-2310(94)90093-0), 1994.  
695  
696 Perrone, M. G., Carbone, C., Faedo, D., Ferrero, L., Maggioni, A., Sangiorgi, G., and Bolzacchini,  
697 E.: Exhaust emissions of polycyclic aromatic hydrocarbons, n-alkanes and phenols from vehicles  
698 coming within different European classes, *Atmos. Environ.*, 82, 391-400,  
699 <https://doi.org/10.1016/j.atmosenv.2013.10.040>, 2014.  
700  
701 Rogge, W. F., Hildemann, L. M., Mazurek, M. A., and Cass, G. R.: Sources of fine organic aerosol.  
702 9. Pine, oak, and synthetic log combustion in residential fireplaces, *Environ. Sci. Technol.*, 32, 13-  
703 22, <http://www.doi.org/10.1021/es960930b>, 1998.  
704  
705  
706 Ruehl, C. R., Nah, T., Isaacman, G., Worton, D. R., Chan, A. W. H., Kolesar, K. R., Cappa, C. D.,  
707 Goldstein, A. H., and Wilson, K. R.: The influence of molecular structure and aerosol phase on the  
708 heterogeneous oxidation of normal and branched alkanes by OH, *J. Phys. Chem. A.*, 117, 3990-  
709 4000, <http://www.doi.org/10.1021/jp401888q>, 2013.  
710

711 Schauer, J. J., Kleeman M. J., Cass, G. R., and Simoneit, B. R. T.: Measurement of emissions  
712 from air pollution sources. 2. C1 through C30 organic compounds from medium duty diesel trucks,  
713 Environ. Sci. Technol., 33, 1578-1587, 10.1021/es980081n, 1999a.  
714  
715 Schauer, J. J., Kleeman, M. J., Cass, G. R., and Simoneit, B. R. T.: Measurement of emissions from  
716 air pollution sources. 1. C1 through C29 organic compounds from meat charbroiling, Environ. Sci.  
717 Technol., 33, 1566-1577, <http://www.doi.org/10.1021/es980076j>, 1999b.  
718  
719 Schauer, J. J., Kleeman, M. J., Cass, G. R., and Simoneit, B. R. T.: Measurement of emissions from  
720 air pollution sources. 3. C1–C29 organic compounds from fireplace combustion of wood, Environ.  
721 Sci. Technol., 35, 1716-1728, <http://www.doi.org/10.1021/es001331e>, 2001.  
722  
723 Schauer, J. J., Kleeman, M. J., Cass, G. R., and Simoneit, B. R. T.: Measurement of emissions from  
724 air pollution sources. 4. C1–C27 organic compounds from cooking with seed oils, Environ. Sci.  
725 Technol., 36, 567-575, <http://www.doi.org/10.1021/es002053m>, 2002a.  
726  
727 Schauer, J. J., Kleeman, M. J., Cass, G. R., and Simoneit, B. R. T.: Measurement of emissions from  
728 air pollution sources. 5. C1–C32 organic compounds from gasoline-powered motor vehicles,  
729 Environ. Sci. Technol., 36, 1169-1180, <http://www.doi.org/10.1021/es0108077>, 2002b.  
730  
731 Schilling Fahnestock, K. A., Yee, L. D., Loza, C. L., Coggon, M. M., Schwantes, R., Zhang, X.,  
732 Dalleska, N. F., and Seinfeld, J. H.: Secondary organic aerosol composition from C12 alkanes, J.  
733 Phys. Chem. A., 119, 4281-4297, <http://www.doi.org/10.1021/jp501779w>, 2015.  
734  
735 Simoneit, B. R. T., Cox, R. E., and Standley, L. J.: Organic matter of the troposphere - IV. Lipids in  
736 harmattan aerosols of Nigeria, Atmos. Environ., 22, 983-1004, [https://doi.org/10.1016/0004-](https://doi.org/10.1016/0004-6981(88)90276-4)  
737 [6981\(88\)90276-4](https://doi.org/10.1016/0004-6981(88)90276-4), 1967.  
738  
739 UK-Air, <https://uk-air.defra.gov.uk>, last accessed 16 December 2018.  
740  
741 Wang, W., Massey Simonich, S. L., Wang, W., Giri, B., Zhao, J., Xue, M., Cao, J., Lu, X. and Tao,  
742 S.: Atmospheric polycyclic aromatic hydrocarbon concentrations and gas/particle partitioning at  
743 background, rural village and urban sites in the North China Plain, Atmos. Res., 99, 197-206, 2011.  
744  
745 Yee, L. D., Craven, J. S., Loza, C. L., Schilling, K. A., Ng, N. L., Canagaratna, M. R., Ziemann, P.  
746 J., Flagan, R. C., and Seinfeld, J. H.: Secondary organic aerosol formation from low-NO<sub>x</sub>  
747 photooxidation of dodecane: Evolution of multigeneration gas-phase chemistry and aerosol  
748 composition, J. Phys. Chem. A., 116, 6211-6230, <http://www.doi.org/10.1021/jp211531h>, 2012.  
749  
750 Zhang, H., Worton, D. R., Shen, S., Nah, T., Isaacman-VanWertz, G., Wilson, K. R., and Goldstein,  
751 A. H.: Fundamental time scales governing organic aerosol multiphase partitioning and oxidative  
752 aging, Environ. Sci. Technol., 49, 9768-9777, <http://www.doi.org/10.1021/acs.est.5b02115>, 2015.  
753



754 Zhao, Y., Hu, M., Slanina, S., and Zhang, Y.: The molecular distribution of fine particulate organic  
755 matter emitted from Western-style fast food cooking, *Atmos. Environ.*, 41, 8163-8171,  
756 <http://dx.doi.org/10.1016/j.atmosenv.2007.06.029>, 2007a.  
757  
758 Zhao, Y., Hu, M., Slanina, S., and Zhang, Y.: Chemical compositions of fine particulate organic  
759 matter emitted from Chinese cooking, *Environ. Sci. Technol.*, 41, 99-105,  
760 <http://www.doi.org/10.1021/es0614518>, 2007b.  
761  
762 Ziemann, P. J.: Effects of molecular structure on the chemistry of aerosols formation from the  
763 OH-radical-initiated oxidation of alkanes and alkenes, *Intl. Rev. Phys. Chem.*, 30, 161-195,  
764 <https://doi.org/10.1080/0144235X.2010.550728>, 2011.  
765  
766  
767

768 **TABLE LEGENDS**

769

770 Table 1. The carbon preference index (CPI) and  $C_{max}$  for n-alkanals, n-alkan-2-ones, and  
771 n-alkan-3-ones in this study and published data.

772

773 Table 2. Percentages of particle phase form and the partitioning coefficient  $K_p$ .

774

775 **FIGURE LEGENDS**

776

777 Figure 1. Map of the sampling sites. RU-Regents University (15 m above ground); WM-  
778 University of Westminster (20 m above ground); EL-Eltham; MR-Marylebone Road  
779 (south side).

780

781 Figure 2. Time series of particle-bound  $\Sigma$ n-alkanals,  $\Sigma$ n-alkan-2-ones and  $\Sigma$ n-alkan-3-ones at  
782 RU, WM, EL, and MR sites.

783

784 Figure 3. The average total concentration of particle-bound n-alkanals ( $C_8$ - $C_{20}$ ), n-alkan-2-ones  
785 ( $C_8$ - $C_{26}$ ), and n-alkan-3-ones ( $C_8$ - $C_{19}$ ), for each sampling period and site. The error bars  
786 indicate one standard deviation.

787

788

789 Figure 4. The molecular distribution of particle-bound carbonyl compounds at four sites (RU,  
790 WM, EL, and MR).

791

792

793

Table 1. The carbon preference index (CPI) and  $C_{max}$  for n-alkanals, n-alkan-2-ones, and n-alkan-3-ones in this study and published data.

Location Sampling site	Sampling period	n-alkanals		n-alkan-2-ones		n-alkan-3-ones		Reference
		CPI	$C_{max}$	CPI	$C_{max}$	CPI	$C_{max}$	
RU, surrounded by Regent's Park, 15 m above ground	23 Jan - 19 Feb	0.52	C <sub>8</sub>	1.23	C <sub>19</sub>	1.30	C <sub>17</sub>	Present study
WM, 20 m above ground	24 Jan - 20 Feb	0.41	C <sub>8</sub>	0.99	C <sub>20</sub>	1.26	C <sub>17</sub>	Present study
EL, suburb of London	23 Feb - 21 Mar	0.71	C <sub>8</sub>	1.57	C <sub>20</sub>	1.04	C <sub>16</sub>	Present study
MR, adjacent to Marylebone road	22 Mar - 18 Apr	1.07	C <sub>8</sub>	0.57	C <sub>16</sub>	1.12	C <sub>16</sub>	Present study
Athens, Athinas St. Urban roadside	August March	1.49	C <sub>15</sub> , C <sub>17</sub>	1.09 3.26	C <sub>18</sub> , C <sub>21</sub> , C <sub>19</sub> C <sub>21</sub> , C <sub>19</sub> , C <sub>20</sub>			(Andreou and Rapsomanikis, 2009)
Athens, AEDA, Urban, 20 m above ground	March			2.41	C <sub>19</sub> , C <sub>18</sub> , C <sub>20</sub>			(Andreou and Rapsomanikis, 2009)
Heraklion, Greece Urban 15 m above ground	Spring /summer	0.80–1.40	C <sub>26</sub> , C <sub>28</sub>	1.30–1.80	C <sub>23</sub> , C <sub>29</sub> , C <sub>31</sub>			(Gogou et al., 1996)
Vancouver, Canada Roadway tunnel				1.33	C <sub>17</sub> , C <sub>19</sub>			(Cheng et al., 2006)
Aveiro, Portugal Suburban	Summer Winter		C <sub>22</sub> , C <sub>23</sub> , C <sub>26</sub>		C <sub>26</sub> , C <sub>28</sub> , C <sub>30</sub>			(Oliveira et al., 2007)
K-Puszt, Hungary	Summer		C <sub>24</sub> , C <sub>26</sub> , C <sub>28</sub>		C <sub>24</sub> , C <sub>26</sub> , C <sub>28</sub>			

Table 2. Percentages of particle phase form and the partitioning coefficient  $K_p$  ( $m^3 \mu g^{-1}$ ).

	RU						WM					
	n-alkanals		n-alkan-2-ones		n-alkan-3-ones		n-alkanals		n-alkan-2-ones		n-alkan-3-ones	
	%	$K_p$	%	$K_p$	%	$K_p$	%	$K_p$	%	$K_p$	%	$K_p$
<b>C<sub>8</sub></b>	82.9	1.16E-04	18.4	5.37E-06	23.9	7.47E-06	80.2	9.09E-05	13.3	3.43E-06	34.1	1.16E-05
<b>C<sub>9</sub></b>	69.2	5.37E-05	14.5	4.03E-06	16.6	4.74E-06	60.5	3.43E-05	15.6	4.16E-06	28.7	9.05E-06
<b>C<sub>10</sub></b>	75.3	7.27E-05	13.6	3.77E-06	7.43	1.92E-06	82.1	1.03E-04	14.4	3.77E-06	23.3	6.82E-06
<b>C<sub>11</sub></b>	45.5	1.99E-05	21.4	6.49E-06	12.8	3.49E-06	62.4	3.72E-05	20.1	5.65E-06	36.3	1.28E-05
<b>C<sub>12</sub></b>	74.8	7.08E-05	25.0	7.96E-06	31.3	1.09E-05	73.7	6.29E-05	28.8	9.07E-06	22.7	6.60E-06
<b>C<sub>13</sub></b>	82.9	1.15E-04	61.0	3.74E-05	35.4	1.31E-05	82.2	1.04E-04	48.9	2.14E-05	62.5	3.74E-05
<b>C<sub>14</sub></b>	82.8	1.15E-04	49.5	2.34E-05	35.5	1.31E-05	75.8	7.04E-05	31.8	1.05E-05	25.6	7.74E-06
<b>C<sub>15</sub></b>	99.5	5.01E-03	84.1	1.26E-04	50.5	2.44E-05	*		85.0	1.27E-04	68.5	4.87E-05
<b>C<sub>16</sub></b>	*		91.4	2.53E-04	70.3	5.64E-05	*		89.6	1.93E-04	91.7	2.47E-04
<b>C<sub>17</sub></b>	*		91.5	2.55E-04	*		*		85.9	1.36E-04	91.5	2.42E-04
<b>C<sub>18</sub></b>	*		94.1	3.80E-04	*		*		84.8	1.26E-04	99.4	4.02E-03
<b>C<sub>19</sub></b>	*		99.1	2.69E-03			*		*			
<b>C<sub>20</sub></b>	*		*				*		*			
<b>C<sub>21</sub></b>			*						*			
<b>C<sub>22</sub></b>			*						*			
<b>C<sub>23</sub></b>			*						*			
<b>C<sub>24</sub></b>			*						*			
<b>C<sub>25</sub></b>			*						*			
<b>C<sub>26</sub></b>			*						*			

	EI						MR					
	n-alkanals		n-alkan-2-ones		n-alkan-3-ones		n-alkanals		n-alkan-2-ones		n-alkan-3-ones	
	%	K <sub>p</sub>	%	K <sub>p</sub>	%	K <sub>p</sub>	%	K <sub>p</sub>	%	K <sub>p</sub>	%	K <sub>p</sub>
C <sub>8</sub>	92.7	6.53E-04	24.9	1.72E-05	31.9	2.43E-05	90.0	2.94E-04	28.2	1.28E-05	43.0	2.46E-05
C <sub>9</sub>	92.2	6.16E-04	38.0	3.18E-05	44.4	4.15E-05	89.9	2.89E-04	27.0	1.20E-05	39.1	2.09E-05
C <sub>10</sub>	90.5	4.96E-04	47.6	4.70E-05	47.0	4.59E-05	91.7	3.62E-04	61.1	5.12E-05	20.4	8.33E-06
C <sub>11</sub>	87.0	3.47E-04	72.3	1.35E-04	81.9	2.34E-04	87.4	2.26E-04	50.2	3.28E-05	33.1	1.61E-05
C <sub>12</sub>	92.9	6.73E-04	83.4	2.60E-04	66.4	1.02E-04	93.0	4.30E-04	88.5	2.51E-04	28.1	1.28E-05
C <sub>13</sub>	95.6	1.12E-03	82.2	2.40E-04	65.7	9.92E-05	96.1	8.04E-04	87.7	2.33E-04	46.2	2.79E-05
C <sub>14</sub>	91.4	5.52E-04	90.3	4.80E-04	59.1	7.48E-05	95.2	6.51E-04	95.9	7.61E-04	72.0	8.38E-05
C <sub>15</sub>	96.7	1.53E-03	94.5	8.98E-04	84.4	2.80E-04	*		96.9	1.02E-03	83.8	1.69E-04
C <sub>16</sub>	*		96.7	1.41E-03	89.0	4.18E-04	*		96.4	8.70E-04	88.0	2.38E-04
C <sub>17</sub>	*		95.1	1.00E-03	81.5	2.28E-04	*		96.0	7.73E-04	88.0	2.39E-04
C <sub>18</sub>	*		64.6	9.44E-05	85.0	2.93E-04	*		92.5	4.04E-04	*	
C <sub>19</sub>	*		*				*		*		*	
C <sub>20</sub>	*		*				*		*		*	
C <sub>21</sub>			*						*		*	
C <sub>22</sub>			*						*		*	
C <sub>23</sub>			*						*		*	
C <sub>24</sub>									*		*	

\* For compounds marked with an asterisk, the particulate phase was quantified, but the vapour was below detection limit, and hence K<sub>p</sub> is undefined.

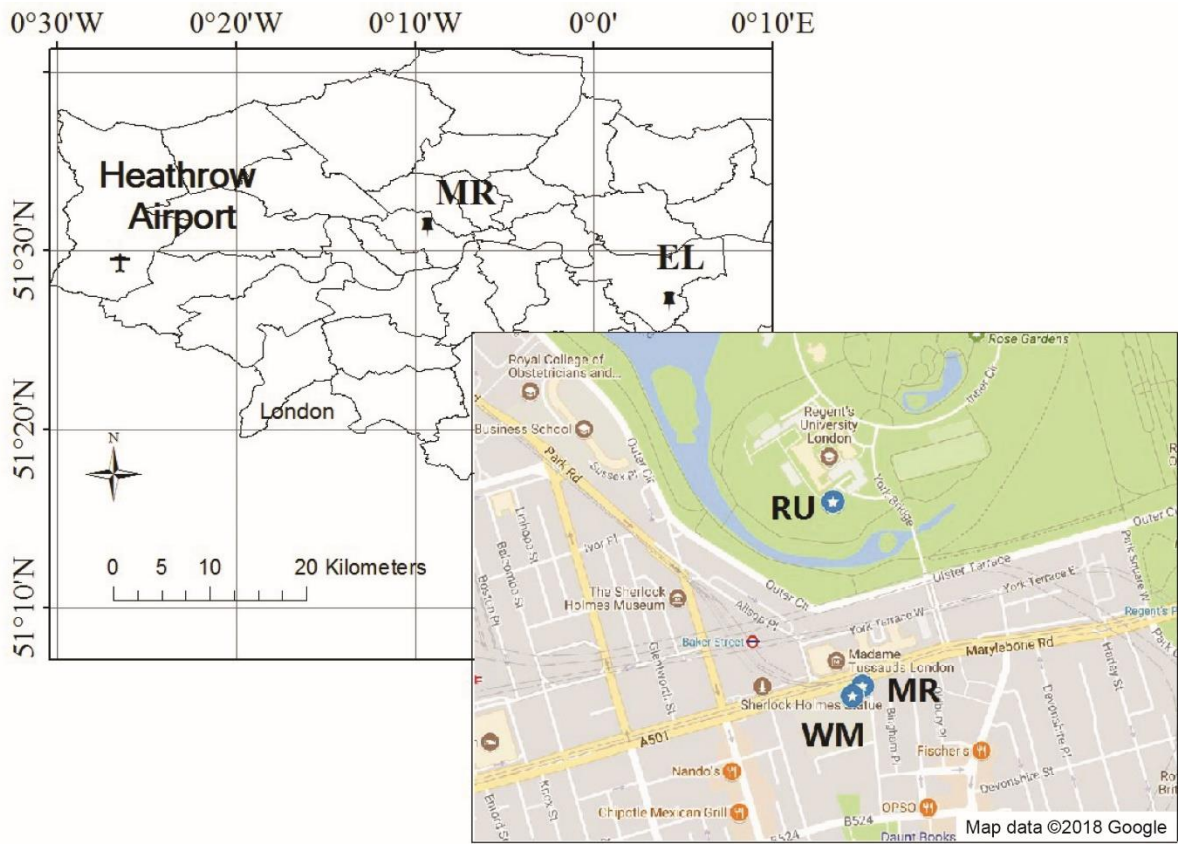


Fig. 1. Map of the sampling sites. RU-Regents University (15 m above ground); WM-University of Westminster (20 m above ground); EL-Eltham; MR-Marylebone Road (south side).

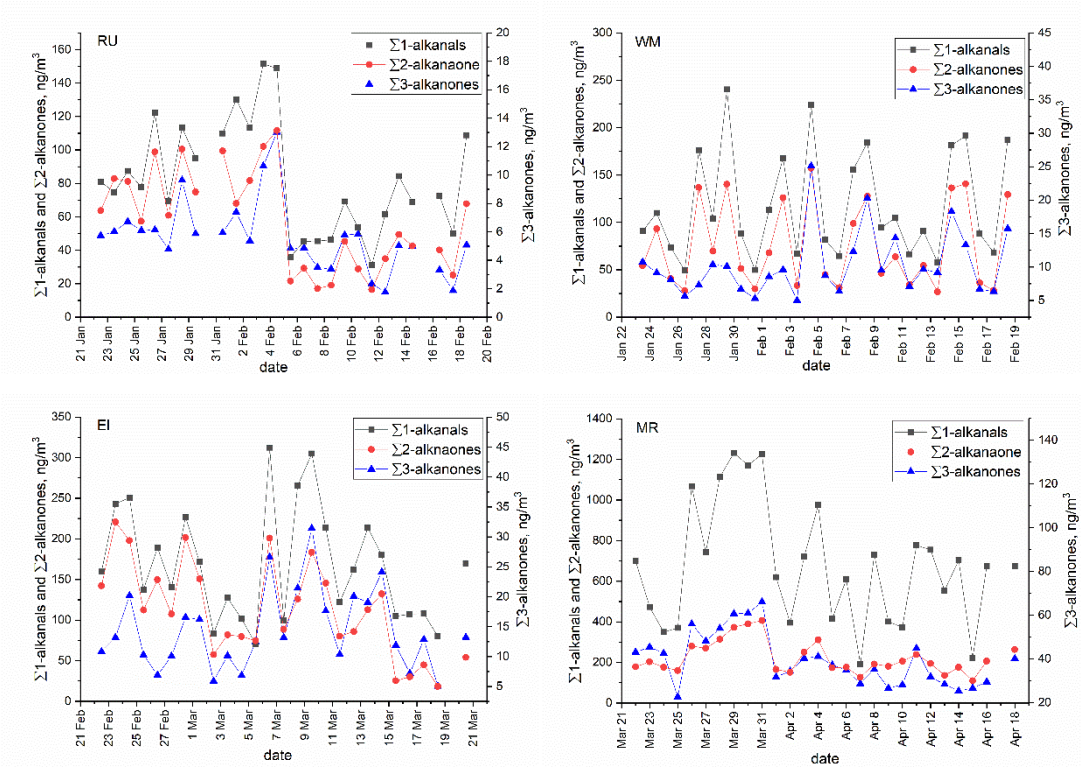


Fig. 2. Time series of particle-bound  $\Sigma n$ -alkanals,  $\Sigma n$ -alkan-2-ones and  $\Sigma n$ -alkan-3-ones at RU, WM, EL, and MR sites.

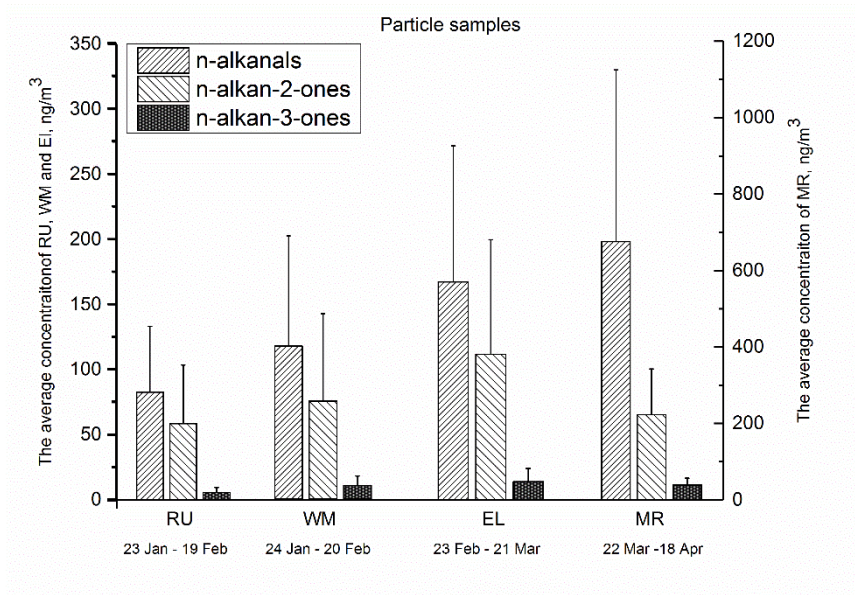


Fig. 3. The average total concentration of particle-bound n-alkanals (C<sub>8</sub>-C<sub>20</sub>), n-alkan-2-ones (C<sub>8</sub>-C<sub>26</sub>), and n-alkan-3-ones (C<sub>8</sub>-C<sub>19</sub>), for each sampling period and site. The error bars indicate one standard deviation.





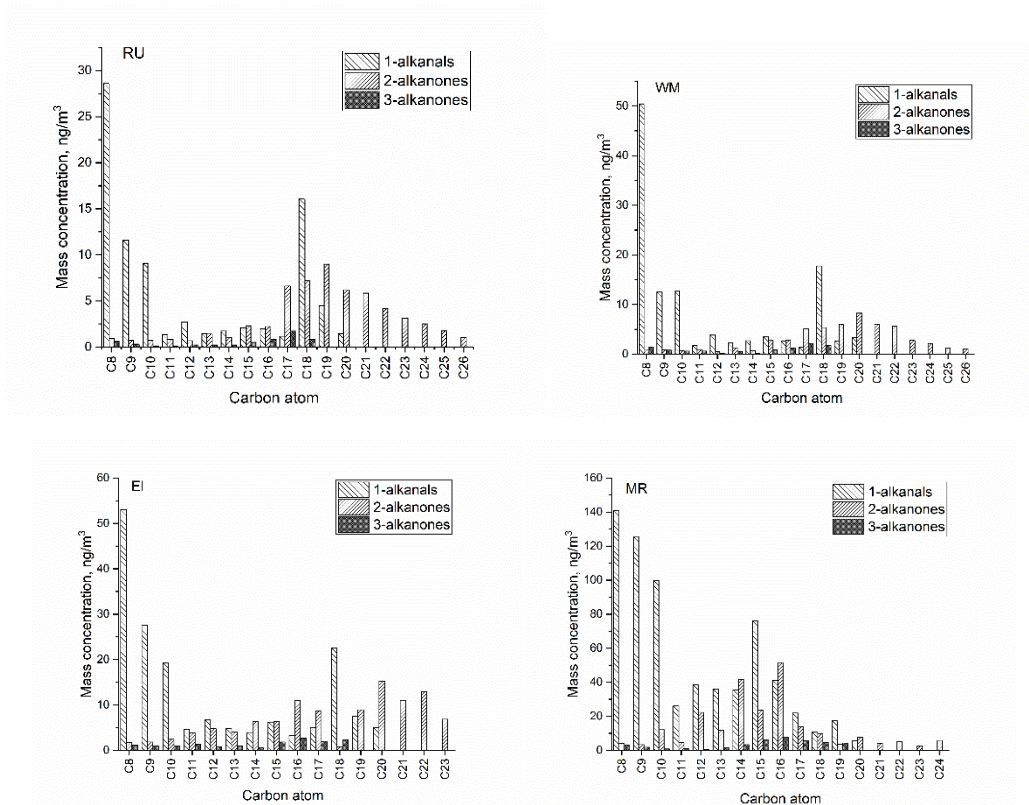


Fig. 4. The molecular distribution of particle-bound carbonyl compounds at four sites (RU, WM, EL, and MR).